



Influence of Waste Tire Rubber Particles Size on the Microstructural, Mechanical, and Acoustic Insulation Properties of 3D-Printable Cement Mortars

Matteo Sambucci^{1,2}, Marco Valente^{1,2*}

¹ Department of Chemical and Material Engineering, Sapienza University of Rome, 00184 Rome, Italy.

² INSTM Reference Laboratory for Engineering of Surface Treatments, Department of Chemical and Material Engineering, Sapienza University of Rome, 00184 Rome, Italy.

Received 05 February 2021; Revised 09 April 2021; Accepted 05 May 2021; Published 01 June 2021

Abstract

3D printing technologies of construction materials are gaining ground in the building industry. As well documented in the literature, these advanced manufacturing methodologies aim to reduce work-related injuries and materials waste, enhancing architectural flexibility which would enable more sophisticated designs for engineering and aesthetic purposes. In this framework, the development of functional and eco-sustainable printable materials represents an extremely attractive challenge for research, promoting digital fabrication to reach its maximum cost-effective and technological potentials. The use of recycled tire rubber particles in 3D printable Portland-based compounds is an exclusive contribution in this field. This line of research aims to integrate the well-known engineering performances of rubber-cement materials with the advanced peculiarities of additive manufacturing methodologies. As an innovative contribution, the authors propose here a detailed study on the possible relationship between rubber particle size and technological properties of the 3D printable mix. Specifically, two groups of continuous size grading polymer aggregates (0-1 mm rubber powder and 1-3 mm rubber granules as fine and coarse fractions, respectively) were analyzed in terms of impact on rheology, print quality, microstructure, mechanical properties, and acoustic insulation performance. Concerning the print quality, rubber aggregates altered the fluidity of the fresh mix, improving the adhesion between the printed layers and therefore enhancing the mechanical isotropy in the post-hardening sample. A remarkable influence of the rubber gradation on the compounds' behaviour was found in hardened properties. By comparing the rubberized compounds, the fine polymer fraction shows greater interfacial cohesion with the cement paste. However, more significant mechanical strength loss was found due to a greater reduction in density and increased porosity degree. On the other hand, mortars doped with larger rubber particles tend to have a higher unit weight, finest pore distribution, minor mechanical strength drop, and higher ductility but worse interface binding with the matrix. Regarding the acoustic insulation properties, a proper balance between rubber powder and granules in the mixes allows to obtain comparable/superior performance compared to plain mortar but the effect of the aggregate size is strongly dependent on the sound frequency range investigated. Future findings revolve around applicability studies of these formulations in civil and architectural fields, benefiting from the design flexibility of 3D printing.

Keywords: 3D Printing; Tire Recycling; Rubber Particle Size; Print Quality; Microstructural Investigation; Mechanical Properties; Sound Insertion Loss.

* Corresponding author: marco.valente@uniroma1.it

<http://dx.doi.org/10.28991/cej-2021-03091701>



© 2021 by the authors. Licensee C.E.J, Tehran, Iran. This article is an open access article distributed under the terms and conditions of the Creative Commons Attribution (CC-BY) license (<http://creativecommons.org/licenses/by/4.0/>).

1. Introduction

Digital manufacturing, such as 3D printing, is one of the most advanced fabrication methodologies in the field of the construction industry, with prospects of revolutionizing the civil and architectural sectors. In the past few decades, a rise in interest towards 3D printing techniques can be mainly attributed to several technological-environmental benefits, listed below [1-4]:

- Targeted and optimized procurement of building materials;
- Wastage reduction;
- Reduction of dangerous manual work and injuries on the construction site;
- Workforce reconversion: traditional labor will be replaced by highly skilled operators programming the printer machines from safe office spaces;
- More architecture freedom: this technology permits design for structural optimization because of its ability to create complex structures without additional labor and cost.

Currently, the extrusion-based printing process is the most explored additive manufacturing option in academia and industry [1, 5]. Similarly to fused deposition modeling (FDM), a visco-plastic cementitious material is extruded out of a deposition nozzle that prints the cement layers. The nozzle is mounted to a robotic motion system and its shape and size are closely related to the characteristics of the desired structure and the size of the aggregates. A pumping system allows the flow of printable material from the mixing unit to the extruder, where it is subsequently released. Starting from a 3D CAD model, the final object is built layer-by-layer using the pre-defined coordinates and the given printing parameters (deposition rate, infill, and layer thickness). Mixture's rheology is a crucial aspect in obtaining a high-quality printing process and a hardened material free of structural defects. Extrudability (the ability of the material to be deposited regularly and without interruptions in the extrusion system), buildability (the ability of the printed layers to hold the subsequent layers on top of them without collapsing phenomena), and inter-layer adhesion (internal compaction of the material due to the correct cohesion between the printed layers) are considered key indicators about the print quality. In this regard, the fluidity and stiffness of the compounds should be properly balanced to meet the requirements described above [1, 5-6].

To enhance the sustainability of 3D printing processes in the construction sector, an attractive challenge for researchers concerns the development of "green" printable cementitious materials based on the use of industrial waste as raw materials to replace traditional virgin aggregates [4, 7]. The present research aims to investigate the printability requirements, the physical-mechanical properties, and the acoustic insulation behaviour of rubber-cement mortars (RCMs) obtained by total replacement of sand with polymer aggregates deriving from end-of-life tires (ELTs). The replacement of mineral materials by recycled rubber in the printable material creates a new avenue for ELTs and reduces the demand for natural resources. As reported by Roychand et al. [8], 1 billion/year waste tires are accumulated annually, of which >50% are illegally disposed or subjected to highly polluting treatments. This trend has encouraged governments around the world to promote the recycling of ELTs through grinding treatments aimed at obtaining new raw materials. According to European Tyre Recycling Association (ETRA) draft model [9], since 2016, over 1.25 tons/year of tire-derived raw materials were used in various industry proposals, reducing reliance on landfills at a low of 5%. Possible uses of ground rubber include molded products [10], rubberized asphalts with improved acoustic and durability performances [11], and rubber-cement compounds for civil-architectural applications [8]. The inclusion of elastomeric fillers in cementitious matrices may help produce low self-weight structures with cost sustainability, improve the mechanical ductility, enhance the vibro-acoustic damping and the heat insulation behaviour, and increase the chemical-physical durability in terms of porosity reduction, water absorption, and carbonation inertia. However, mechanical strength reduction, due to the poor rubber-cement interface adhesion, represents the weak point of this technology [12-14]. Although many studies on pre-cast concrete mixes modified with recycled tire rubber were proposed, there are no attempts and research activities available on the application of these polymer aggregates in the production of cementitious compounds for 3D printing methods. The objective is to combine the technological functionalities conferred by rubber with the performance of additive manufacturing in terms of design flexibility, structural optimization, and low pollution. Several efforts were already conducted by the authors on this topic, involving preliminary printability and print quality studies to explore the potential of incorporating recycled tire rubber particles into printable cementitious mixes [5, 7, 13], experimental characterization on durability analysis [13], the effect of rubber-based modification on thermal insulation properties [7, 15], first mechanical investigations and modelling [5, 7, 15, 16]. From the perspective of rational production of secondary raw materials by the tire recycling companies, economic impact and material performance, the novel purpose of the present study is to deepen in detail the influence of rubber particle size on the fresh and hardened properties of printable mortars. The manufacturing cost and energy consumption of the tire grinding process vary greatly depending on particle size gradation. These aspects must be carefully considered to encourage the sustainability of the entire

production cycle, and therefore an evaluation of the interaction between rubber particle size and material performance can provide valuable information for both manufacturers and researchers.

Specifically, in this work, the effect of rubber particle size on the rheological, microstructural, mechanical, and acoustic properties of RCMs was investigated. 0-1 mm rubber powder (RP) and 1-3 mm rubber granules (RG) were used as fine and coarse aggregates in the mixes, respectively. First, a detailed characterization of the polymer aggregates is reported to investigate the influence of the gradation on the fresh properties of the mixes and the physico-mechanical behaviour of RCMs. Then, the suitability of proposed compounds for 3D printing fabrication was validated by printability tests, consisting of the manufacture of 6-layers slabs and subsequent assessment of specific print quality requirements. Finally, to evaluate how the rubber-based modification affects the mortars' features, a series of experimental analysis, including, scanning electron microscopy (SEM), pore size analysis by optical microscopy (OM), cube compressive strength, flexural test, and sound insertion loss (SIL) measurements were conducted on specimens extracted from the printed slabs. Although some similarities with previous publications in the literature, this manuscript presents a more exhaustive and rigorous description of the mechanisms underlying the relationship between rubber characteristics (gradation, morphology, replacement level) and resulting material behavior.

2. Materials and Methods

2.1. Tire Rubber Aggregates

The waste rubber particles, obtained by ambient mechanical grinding of ELTs, were sourced from European Tyre Recycling Association (ETRA, Belgium) plants. Two different polymer aggregates were investigated in this work: RP (Figure 1a) which was a fine fraction with grading close to the limestone sand used in this research, and RG (Figure 1b) as coarse fraction.

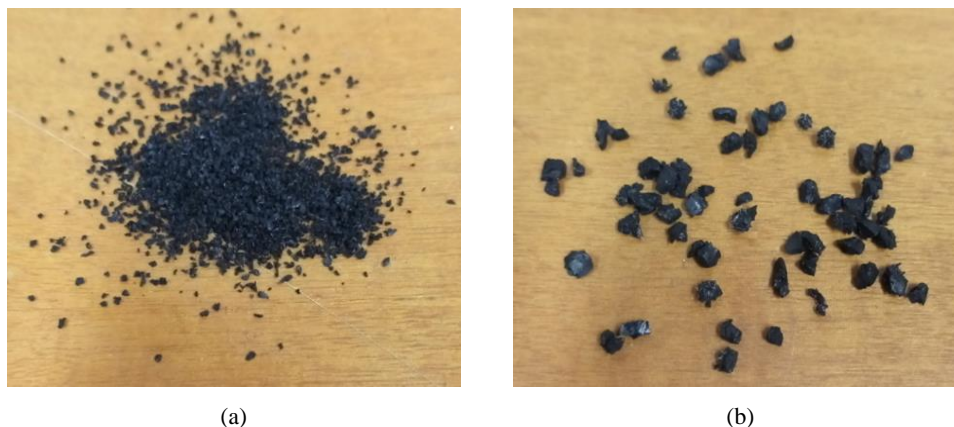


Figure 1. Rubber particles used in this work: (a) 0-1 mm RP; (b) 1-3 mm RG

Experimental sieving analysis (Figure 2 and Table 1), performed in accordance with DIN 66165 standard method [17], revealed 0.425-1 mm range size for RP and 1.7-3 mm range size for RG.

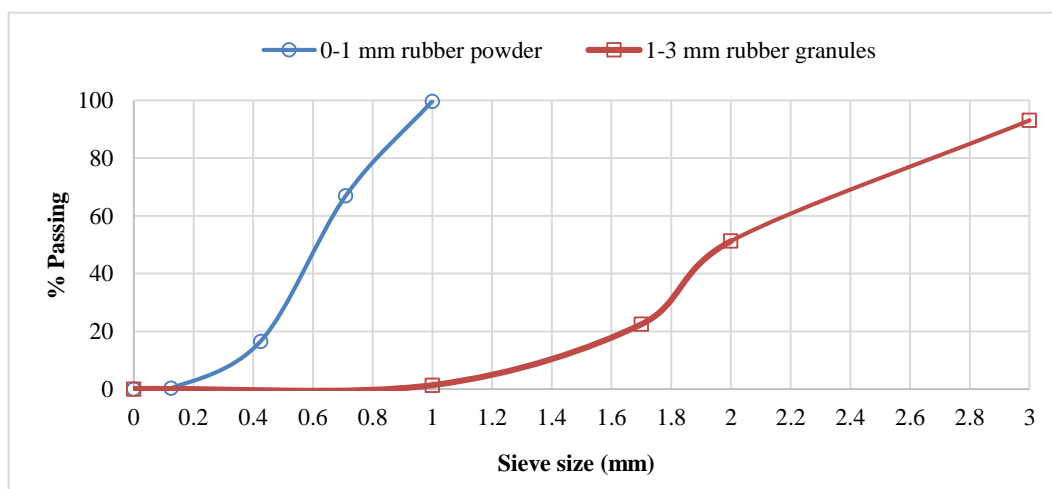
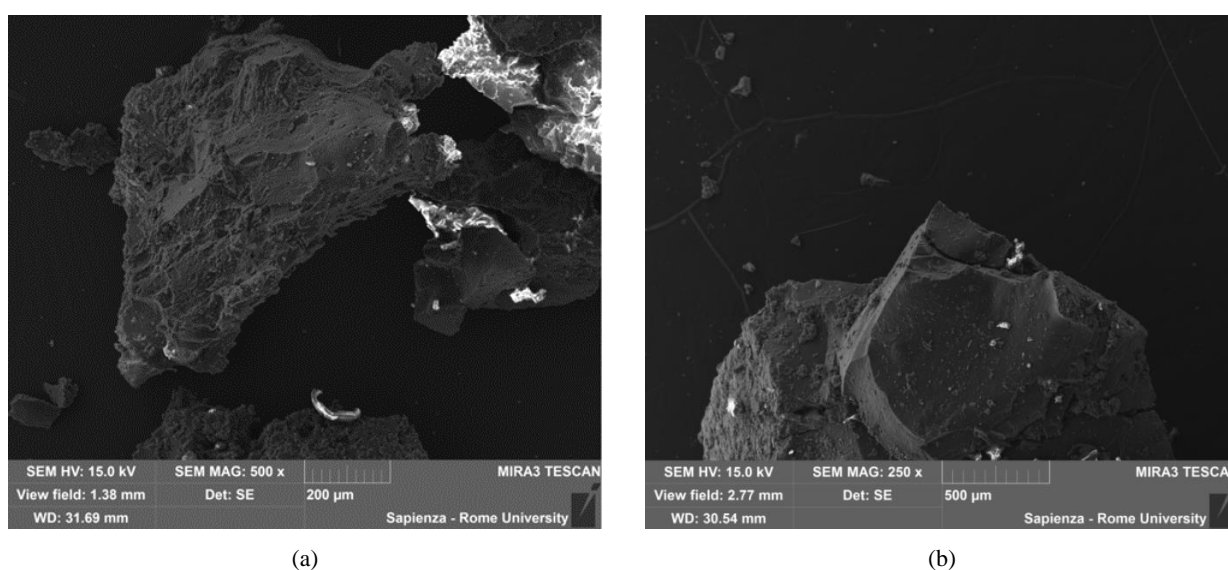


Figure 2. Grading curves of tire rubber aggregates

Table 1. Sieving analysis results of tire rubber aggregates

0-1 mm rubber powder		1-3 mm rubber granules	
Sieve size (mm)	% passing	Sieve size (mm)	% passing
1	99.70	3	99.13
0.710	66.94	2	51.28
0.425	16.55	1.7	22.47
0.125	0.28	1	1.35

The average specific gravity of rubber particles, measured by Micromeritics AccuPyc 1330 He-pycnometer, is 1.2 g/cm³. The morphology and surface texture of rubber particles were inspected by scanning electron microscopy (SEM) analysis. Prior to the examination, rubber samples were fixed on a carbon adhesive tape and then made conductive by graphitization treatment using a Leica EM SCD005 vacuum sputter coater. Secondary-electron (SE) imaging (Figure 3) were collected using a Tescan Mira3 FEG-SEM.

**Figure 3. SEM micrographs of tire rubber particles: (a) RP; (b) RG**

From SEM analysis, it is possible to notice the different surface morphology of the aggregates: RP shows rough and irregular texture, while in RG a smoother and more regular surface is detectable. This is attributable to the shredding treatment. To obtain a greater fineness degree, more grinding cycles are required, resulting in more irregular shaping of the rubber particles [16].

2.2. RCM Mixtures Proportioning

The rubberized compounds were obtained from plain Portland-based mortar (designated as “CTR”) by total volume replacement of the sand with the polymer aggregates. CTR mix is composed of Type I Portland cement (800 kg/m³), limestone sand of 0.4 mm maximum size (1100 kg/m³), and water (300 kg/m³).

Three RCMs (designated as “RP100”, “RP50-RG50”, and “RP25-RG75”) were developed by incorporating the rubber fractions in different proportions: RP100 refers to mix with 100% by volume of RP, RP50-RG50 consists of equal volume content of RP and RG, and RP25-RG75 provides RP and RG in 1:3 proportion ratio. The water amounts were adjusted by trial printability tests aimed to evaluate the correct extrudability and buildability properties of the fresh mixes. The water contents in the rubber-based mortars (260, 250, and 230 kg/m³ in RP100, RP50-RG50, and RP25-RG75, respectively) are lower than CTR mix. According to Lyse’s rule and the typical workability behaviour of cementitious compounds, the larger size and more regular shape of rubber aggregates than sand imply a lower water dosage to reach the same fresh material consistency [13, 18]. This also explains the decreasing trend in the water content when RG content is added in the mixes.

Finally, all the investigated mixes had a fixed content of chemical admixtures (152 kg/m³) to ensure suitable rheology for the printing process. The correct balance of additives is summarized in Table 2.

Table 2. Admixtures content in printable mortars

Admixture	Amount
Silica fume-based thixotropic additive	79 %
Polycarboxylate ether-based superplasticizer	2.6 %
Aliphatic-based water reducing agent	5.2 %
Calcium oxide-based expansive agents	13.2 %

2.3. Specimens Manufacturing and Testing Methods

A custom-made printing system was used to produce the mortar samples for the materials characterization. The apparatus involves a Comau Robotics 3-axis robotic arm (Figure 4a) equipped with a PVC circular nozzle ($\varnothing = 10$ mm). The nozzle is connected to a pressure vessel (4 bar) containing the fresh mix, which is extruded with a constant deposition speed of 33 mm/s. Moderate external vibration was applied to the vessel to ensure adequate compaction of the cement compounds. Starting from a 3D CAD model, 6-layers slabs (230×160×55 mm) were printed for each mix. Ultimaker Cura slicing software was used to generate the GCode file of the object and select the main process parameters. After the printing, the slabs (Figure 4b) were cured for more than 28 days at ambient temperature and, therefore were cut by a diamond circular saw to obtain four types of specimens for the laboratory tests.

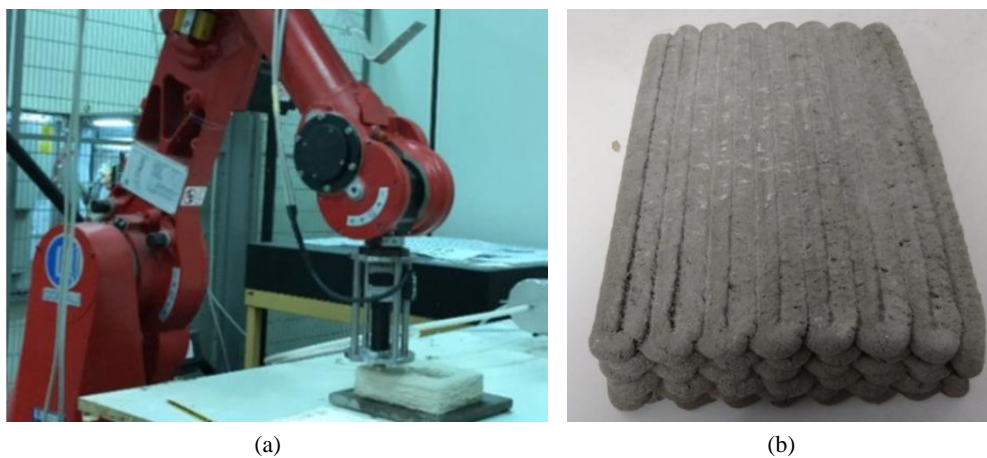


Figure 4. (a) 3D printing system; and (b) rubber-cement slab after 28 days of curing

A flowchart of this research methodology is presented in Figure 5.

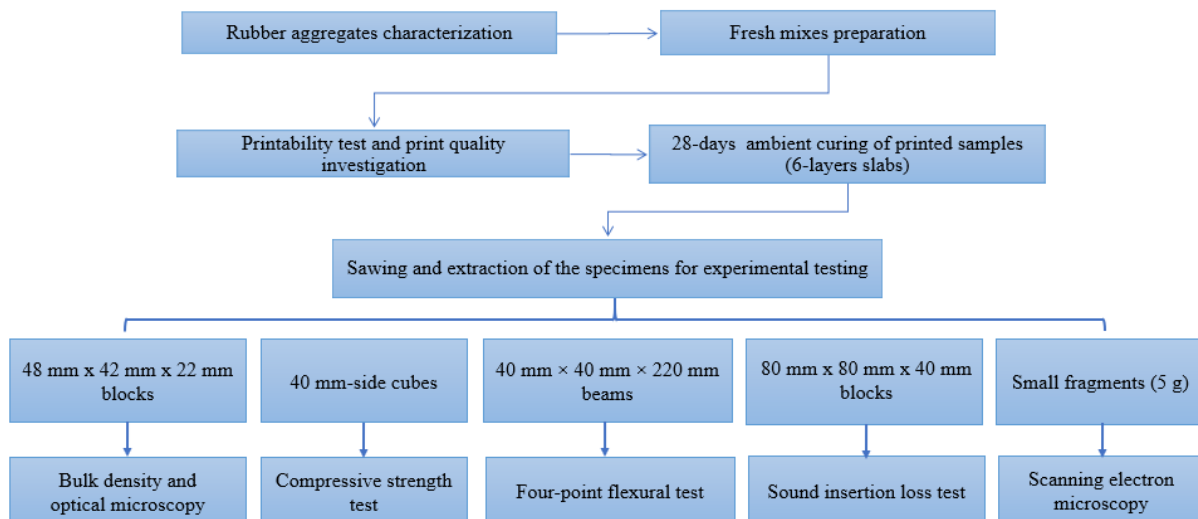


Figure 5. Flowchart of the research methodology conducted in this work

2.3.1. Bulk Density Testing Method

Bulk density (ρ) measurements were conducted in accordance with BS 1881-114 standard method [19] on 48×42×22 mm blocks. After 48 hours of oven-dry treatment (110 °C), the weight and the geometric volume of the samples were determined, then ρ was calculated as mass to volume ratio. For each mix, ρ -result is an average value of four tested specimens.

2.3.2. Mechanical Characterization

To evaluate the compressive strength (σ_c) of printed mortars, 40 mm-side cubes were tested in two different load directions, namely Z-direction (load direction perpendicular to printed filaments plane) and X-direction (load direction longitudinal to printed filaments plane). Figure 6a illustrates the orientations of the compressive load with respect to the layered structure of the printed element. Mechanical tests were performed in accordance with ASTM C109/C109M-20a [20], using a Zwick-Roell Z150 machine (150 kN capacity) at a loading rate 1 mm/min. For each loading direction three samples were analysed. A detail of the test is shown in Figure 6b.

Four-point flexural test was conducted following the ASTM C348-20 standard method [21] to measure the flexural strength (σ_f), the Young's modulus (E), and the elongation at break (ϵ) of investigated mortars. 40×40×220 mm beams were tested by a Zwick-Roell Z010 machine (10 kN capacity), using a support span of 180 mm at a loading rate of 1 mm/min. Contrary to compressive test, the specimens were tested by applying the bending load orthogonally to the print plane (Z-direction). Three beams per mix were mechanically investigated under flexural load.

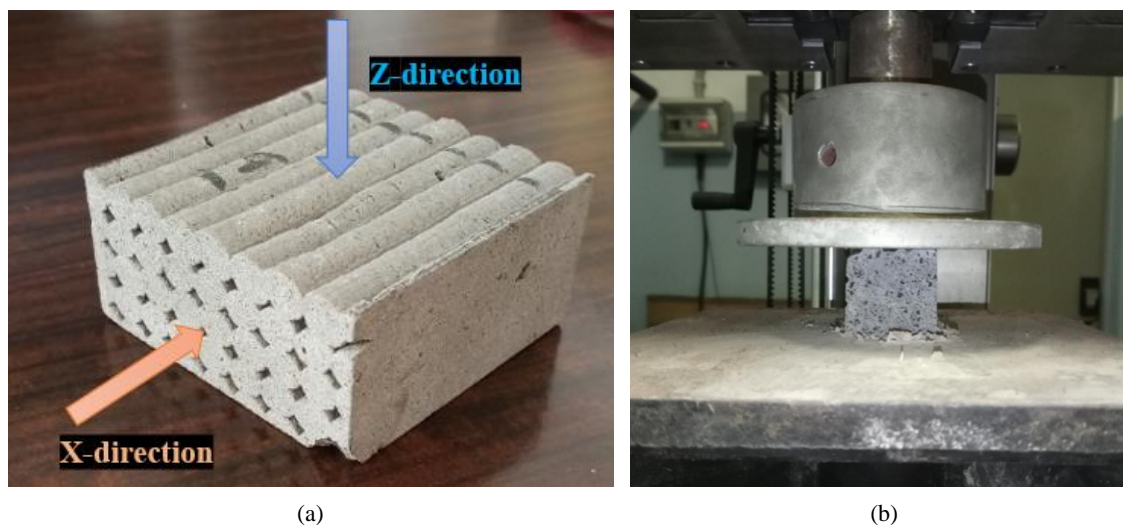


Figure 6. Compressive test on rubber-cement specimens: (a) Spatial orientation of the compressive loads; (b) Experimental configuration

2.3.3. Acoustic Insulation Analysis: Sound Insertion Loss Measurements

The influence of rubber aggregates on acoustic insulation properties of printable mortars was investigated by sound insertion loss (SIL) analysis. The experimental test was performed by using a two-microphone impedance tube (Figure 7) in accordance to ISO 7235 standard method [22]. The tube had an internal diameter of 16 cm, a length of 100 cm, and mounted two ¼" condenser microphones (Behringer ECM800) at a distance of 40 cm for sound insulation measurements. A Behringer MPA30BT loudspeaker, at one end of the tube, generated a Log sweep acoustic signal from 50 Hz to 4000 Hz. The loudspeaker was housed inside an acoustic box filled with sound-absorbing polyurethane foam to ensure the correct sound flow in the duct. A Focusrite Scarlett 2i4 audio interface was used for the processing of audio signals during the experiment. The other end of the tube is sealed with an absorbent termination to minimize unwanted acoustic reflections in the tube. 80 mm x 80 mm x 40 mm blocks were placed in the middle part of the duct between the microphones. Experimental evaluation of SIL-index consists in measuring the sound pressure level gradient between the two microphones with and without the specimen. SIL as a function of the acoustic frequency (f) is calculated as follows (Equation 1):

$$SIL(f) = \Delta L_0(f) - \Delta L_s(f) \quad (1)$$

Where:

$SIL(f)$ is the sound insertion loss as a function of the acoustic frequency [dB];

$\Delta L_0(f)$ is the sound pressure level gradient between the microphones without the sample [dB];

$\Delta L_s(f)$ is the sound pressure level gradient between the microphones with the sample [dB].

For all four investigated mortar, SIL-values in the range 50-4000 Hz was plotted. The data were acquired and processed by Room EQ Wizard software.

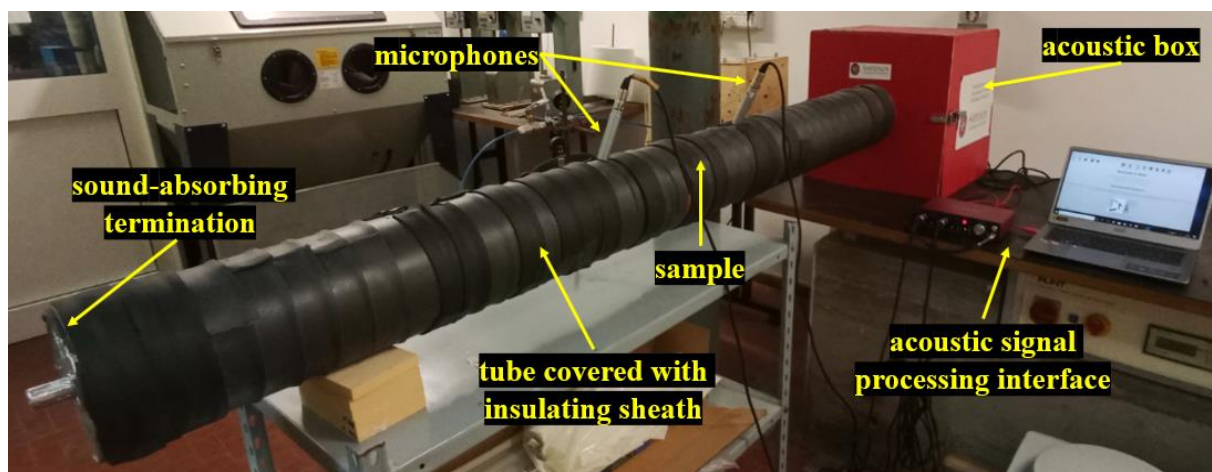


Figure 7. Experimental setup for SIL measurements by two-microphone impedance tube

2.3.4. Microstructural Analysis

Scanning electron microscopy (SEM) investigation was conducted to analyse the effect of particle size on the rubber-cement interface properties of the RCMs. Small fragments of investigated materials (about 5 g) were examined with a Tescan Mira3 FEG-SEM. The specimens were coated with graphite prior to the analysis using the same procedure performed on the granular tire rubber samples (see Section 2.1).

A specific methodology and software were used to investigate the pore structure via digital image analysis. The same test specimens used in ρ measurements were analyzed by a Leica MS5 stereomicroscope. For each formulation, four cross-section images (16x magnification) were acquired by using Lucia Imaging software. The micrographs were analyzed by ImageJ software to obtain the surface characteristics and macro-porosity (100 μ m-1 cm), of the specimens. Considering a representative number of voids, pore size distribution was evaluated by measuring the effective diameter of each void, assuming it to be perfect circle. The corresponding cumulative frequency (based on the number of air pores detected) was computed, according to the following size ranges: $\leq 100 \mu\text{m}$; 100-200 μm ; 200-300 μm ; $\geq 300 \mu\text{m}$.

3. Results and Discussions

3.1. Print Quality Investigation

Mortars' print quality was evaluated considering three printability indicators: a) regular and uninterrupted extrusion of the fresh mix (*extrudability*); b) layer-by-layer stacking capability without collapse (*buildability*); c) printed filaments cohesion (*inter-layer adhesion*). The 3D-printable compounds developed in this study satisfied the abovementioned requirements. However, as can be seen in Figure 8a, all the RCMs exhibited greater structural compaction than CTR mix. As confirmed by previous studies [13, 23], an influence of adding polymer aggregates into cementitious compounds is the improvement in fluidity. The hydrophobic groups in the macromolecular structure of rubber could attract air in the cement paste and incorporate air bubbles during the mixing, by reducing the overall surface tension of the fresh mix. This phenomenon made the paste flow more easily, enhancing the inter-filament bond in the RCM samples. As a consequence of this evidence, the air-entraining performance of rubber is inevitably crucial about specific physical-rheological properties, including viscosity, pore structure, and unit weight [24].

Furthermore, the rubber particles are less water-absorbent than the mineral aggregates, leading to a higher rate of free water in the fresh mixes. During the printing process, surface moisture acts as a cohesive layer for the printed filaments, improving the intermixing of the layers and interfacial adhesion. In the context of extrusion-based digital fabrication, layer-to-layer adhesion is a major factor affecting the integrity of a 3D-printed structure.

In Figure 8b, it is possible to observe a more evident stratification in CTR sample compared to the rubberized one (in this example RP100 sample), where a more homogenous structure occurs. The weak interfacial bond, generally defined as "cold joint", induces pronounced mechanical anisotropy, strength loss, and negatively affects the durability performance of the printed element [25]. In this respect, modification with rubber has proved to be an efficient strategy for improving the structural quality of the material.

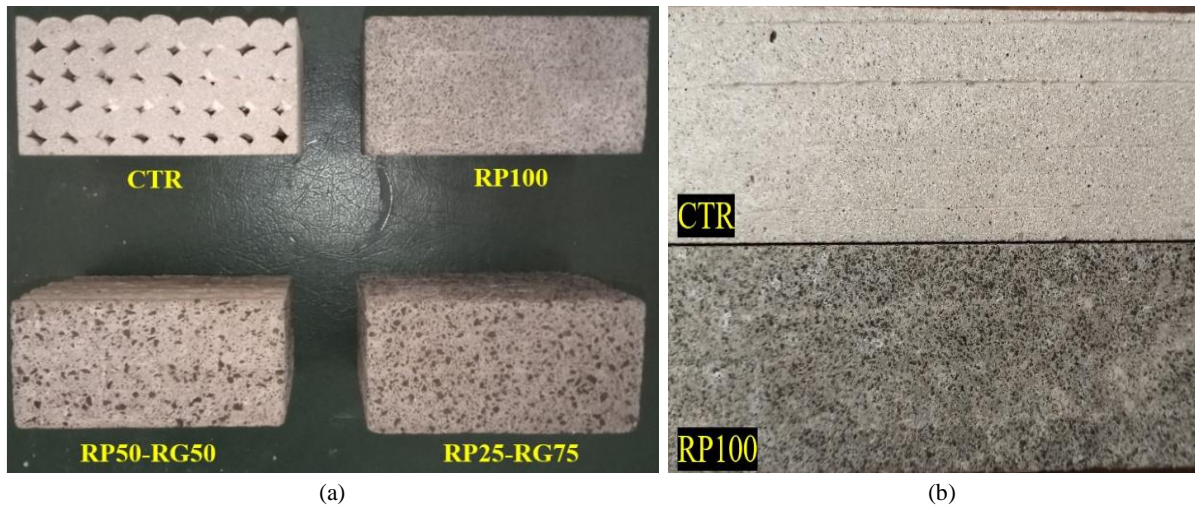


Figure 8. Inter-filament adhesion evaluation (a) and layering (b) in CTR and rubberized samples

3.2. Microstructural Analysis

The interfacial binding efficiency between the rubber aggregates and surrounding cement matrix is shown in the 1kX magnification SEM SE-micrographs (Figure 9) reported below.

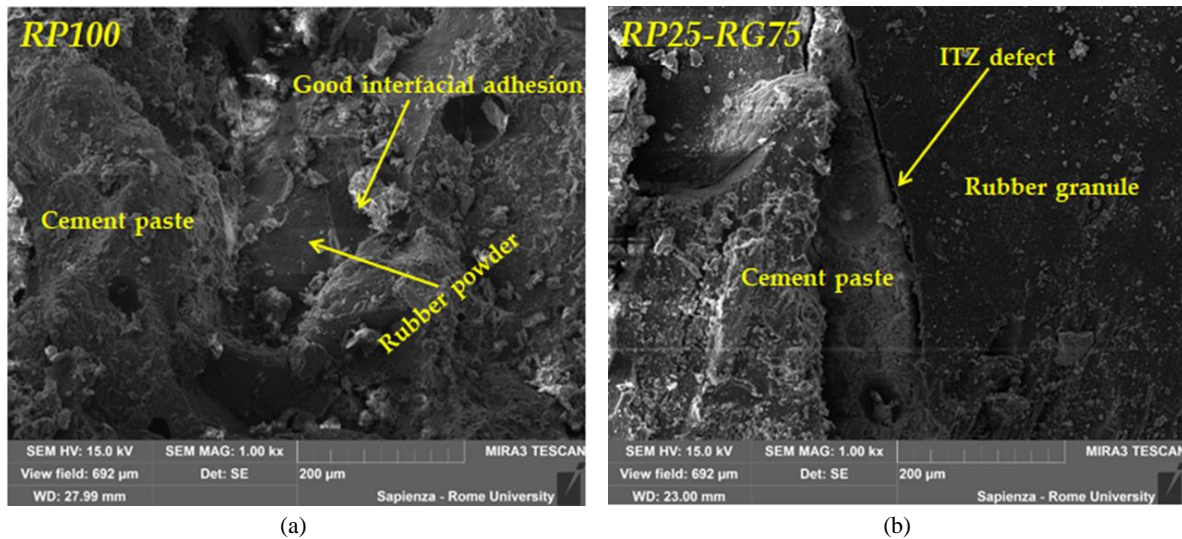


Figure 9. RP-cement (a) and RG-cement (b) interfacial adhesion

As mentioned earlier, the mechanical grinding degree affects the surface morphology of tire rubber particles. As shown in Figure 7b, the coarser polymer fraction has a smaller specific surface area than the finest one, resulting in a weaker cohesion with the cement and porous Interfacial Transition Zones (ITZs). Conversely, the presence of structural “jaggies” in RP, due to their irregular texture, is beneficial about the adhesion with the cement matrix. The relationship between rubber particle morphology and adhesion properties with the cement paste agree the research of Ghizdăveţ et al. [26].

Air bubbles content in cementitious materials results from several factors: accidental incorporation of air in the fresh mix, incomplete compaction of the cement paste, or excessive water dosage. When the material hardening occurs, the air bubbles turn into mechanical weakness elements, causing structural defects and degradation points [27]. Macro-pores and capillary porosity (<10 µm) govern numerous properties of concrete and mortars, such as mechanical strength, elasticity, and permeability [28].

Optical microscopy analysis revealed interesting effects of rubber inclusion on the microstructural characteristics of the cementitious compounds. The major findings are listed below:

- *Air bubbles porosity reduction.* From the optical micrographs (Figure 10), it is possible to qualitatively observe an overall surface porosity reduction in the rubberized compounds compared to CTR sample. The alteration in rheological behaviour when the rubber is incorporated into the cement mixture is the main reason for this trend. First, as well pointed by Sun et al. [29], rubber modification reduces the viscosity and the flow resistance of the

cement paste. Low plastic viscosity promotes the diffusion and the escape of air bubbles from the paste, preventing their retention in the hardening material [30]. Besides, rubber aggregates reduced water content in the cementitious mixes, maintaining proper fresh properties for printing (see Section 2.2). This effect is more pronounced in RG-based mortars, where the concentration of air voids tends to gradually decrease. The influence of water dosage on the material porosity is supported by several literature pieces of research [24, 26]: with the decrease in the water-to-cement (w/c) ratio, the rate of free water that evaporates is lower, implying a reduction in air voids rate.

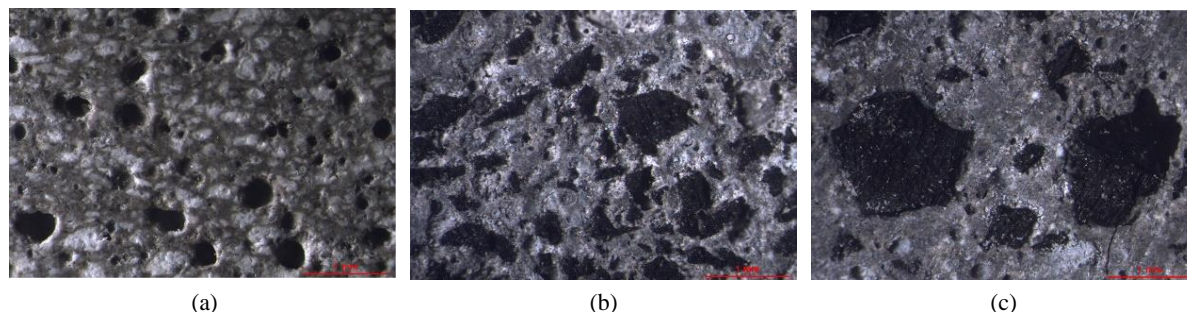


Figure 10. Microstructural analysis by optical microscopy: CTR (a), RP100 (b), and RP25-RG75 (c) samples

- **Pore size reduction.** The influence of rubber on w/c ratio also plays a key role on the pores dimension. This evidence is well demonstrated by the graph in Figure 11. Which highlights the pore size distribution evaluated by imaging analysis.

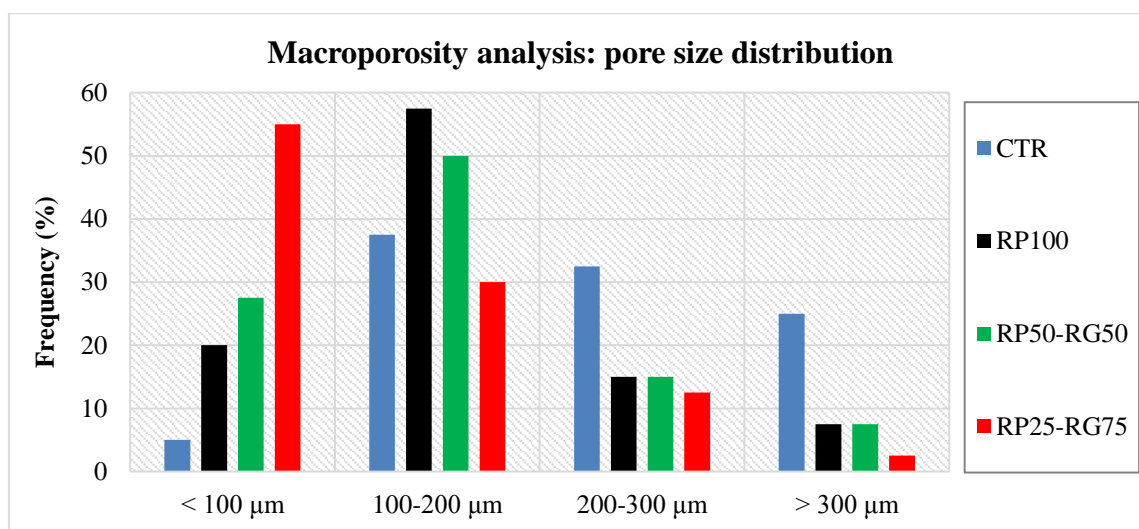


Figure 11. Cumulative pore size distribution for CTR and rubberized mixes

The pores size of CTR sample (w/c ratio = 0.375) is homogeneously distributed in the range from 100 μm up to more 300 μm, with negligible concentration of small voids (< 100 μm). On the other hand, opposite trend can be observed in rubberized mixes. The proportion of pores in RP100 (w/c ratio = 0.325) and RP50-RG50 (w/c ratio = 0.312) is mainly located in 100 – 200 μm range, indicating a less evident contribution of coarse macro-porosity (> 200 μm). The lower w/c ratio formulation, i.e. RP25-RG75 mix (w/c ratio = 0.287), highlighted the predominant contribution of finest porosity. These results are consistent with the literature findings drawn from the relationship between air pores structure and water content in cementitious media [31]. Voids dimension is mainly controlled by water amount: higher w/c ratio results in large pores in the cement matrix. Several studies demonstrated the functionality of finest air bubble porosity on cement materials’ engineering performances. As ascertained by Das and Kondraivendhan [32], smaller size pores enhance the durability of concrete in terms of permeability and hydraulic diffusivity inertia. Neithalath et al. [3] revealed strong influence of air void dimensions on the acoustic properties of enhanced porosity concrete. The reduction in pore size increases the maximum acoustic absorption, as for a propagation medium with small sized pores the frictional losses are high and a considerable portion of the acoustic waves that enter the pore system is dissipated. Remesar et al. [34] studied the effect of pore size gradation on the thermal insulation properties of lightweight concrete. At the same porosity degree, smaller pores own many more reflecting/refracting surfaces of heat flux, preventing the radiative transfer into the material and improving its heat insulation.

The rheology and microstructural properties induced by the rubber inclusions are hypothetically explanatory of the higher inter-layer adhesion revealed in the rubberized samples compared to CTR mix. The low water evaporation rate, due to the reduced w/c ratio and the preferential presence of fine porosity, can be considered a key factor regarding the cohesion between the extruded filaments. Indeed, the maintenance of a certain degree of surface moisture in the printed filaments during the additive process allows a better interface bonding, avoiding the premature hardening of the deposited materials and stiffness mismatches that can create interfacial voids (as clearly observed in the CTR sample). The relationship between inter-layer adhesion of 3D printable cementitious materials and surface humidity degree is well documented in Weng et al. research [35].

3.3. Physical-mechanical Characterization

Table 3 reports the results of the experimental programme based on bulk density and mechanical tests.

Table 3. Physical-mechanical characterization: experimental results

Sample	ρ (kg/m ³)	σ_{cx} (MPa)	σ_{cz} (MPa)	σ_f (MPa)	E (GPa)	ϵ (%)
CTR	1927	63.1	44.1	4.21	5.56	0.05
RP100	1340	14.5	11.6	1.37	1.94	0.37
RP50-RG50	1624	18.9	16.8	2.11	1.89	0.40
RP25-RG75	1468	15.7	11.1	1.58	1.82	0.55

The sand-rubber replacement reduces ρ -values. Unit weight drop can be mainly attributed to the lower specific gravity of the rubber particles than mineral ones, the contribution of ITZ voids, and the variation in the overall porosity depending on w/c ratio [5, 16, 36]. The most relevant density reduction is observable in RP100 mix, where the total incorporation of fine polymeric fraction implies a higher weight content of rubber in the material.

The bulk density trend is in line with the lower σ_c and σ_f in RCMs, which also depend on the weak rubber-cement interface adhesion and the soft properties of polymer fillers, resulting in premature cracking in the surrounding cement matrix. The results of this work are consistent with previous experimental studies [5, 16, 37, 38]. However, two noteworthy findings can be deduced from the compressive strength results.

- Although the sand-rubber replacement level was similar in all the rubberized formulations, by varying the proportion of fine and coarse polymer fraction it is possible to modulate the mechanical strength properties. By reducing the w/c ratio increases the strength of the cement matrix around the rubber particles. This explains the lower mean compressive and flexural strength loss in RP50-RG50 (-50% for σ_f , -70% for σ_{cx} , and -62% for σ_{cz}) and RP25-RG75 (-63% for σ_f , -75% for σ_{cx} , and -75% for σ_{cz}) compared to RP100 (-68% for σ_f , -77% for σ_{cx} , and -74% for σ_{cz}). Furthermore, the contribution of the particle size was considered. In general, the strain capacity is significantly enhanced when rubber particles are added and attributed to the ability of polymer inclusion to reduce stress concentration and delay the coalescence and propagation of micro-cracks [39]. The coarser rubber fraction appears to act more efficiently in terms of crack-arresting properties, resulting in better mechanical behaviour. By comparing the “hybrid” rubber-cement formulations, the divergences in mechanical strength are mainly attributable to the rubber-cement interface properties. As previously discussed, RG involve weaker adhesions with the cement paste (ITZ defects), deleteriously affecting the structural integrity of the sample. This explains the lower strength levels in RP25-RG75 mix compared to RP50-RG50.
- By comparing X and Z-directions mechanical strengths (denoted as σ_{cx} and σ_{cz} , respectively), it is possible to notice a greater convergence in the experimental values of rubberized compounds than CTR one. The rubber-based functionalization reduces the typical mechanical anisotropy of the 3D printed samples, as a result of the great structural compaction and inter-layer adhesion discussed in 3.1 section. The percentage deviation between the σ -values in Z-direction and X-direction was 43% for CTR and 25%, 12.5%, and 41% for RP100, RP50-RG50, and RP25-RG75, respectively. Reducing the post-hardening directional behaviour of 3D-printable cementitious materials is one of the most felt challenges in the field of AM technologies. In terms of design optimization for civil and architectural applications, enhancing mechanical isotropy has positive implications regarding the possibility of exploiting the full potential of digital fabrication. The observed divergences in σ -values measured in different loading directions can be attributable to two aspects: a) the orientation between applied stress and printed filaments; b) the direction-dependent compaction of the extruded material. From Table 3, σ_{cx} demonstrates the best performance under compression, presumably due to the favorable orientation of the filaments for the applied pressure, which allows them to act as a series of columns with high compressive resistance, minimizing the mechanical stress at the weak inter-filament interfaces. A further reflection concerns the non-homogeneous densification that can be detected in a printed structure. The pressure exerted during the extrusion process through the pumping system is higher in the longitudinal direction (extrusion direction) than

the other orientations, maximizing the compaction of the material. Conversely, in the perpendicular direction (Z-direction) the compaction is mainly related to the self-weight of the mortar. Similar remarks can be found in [40, 41].

To appreciate the effect of tire rubber aggregates on the elasto-mechanical properties of the printable mortars, the flexural stress-strain diagram is presented in Figure 12, considering the most representative specimens of each formulation. The addition of tire rubber aggregates significantly changes the deformation capacity of the mortars. In RCMs occurs an average E-value decrease of 95% compared to the neat sample, due to the lower elastic modulus of rubber than sand. For the same rubber-sand replacement levels, there are no significant variations of E with the tire particle size. The reduced modulus improves the deflection properties, prevents the brittle failure of the material, and leads to potential improvement in vibro-acoustic damping [42-43]. The effect of particle size is well evident on the ϵ -properties. The higher the RG content, the higher the material ductility. Reda Taha et al. [44] explained this behaviour by the ability of rubber inclusions to absorb part of the energy the matrix is subjected to, and therefore the rubber-cement material can absorb more mechanical energy before fracturing compared to the neat matrix. Polymer inclusions acted as obstacles to crack initiation and propagation that could have had a preferential path through the mineral aggregates. Therefore, during propagation, cracks must overcome the rubber-cement bond, circumnavigating the polymer particle. This prolongs the propagation path, postponing the failure process in the material [45]. In this context, the coarse fraction has a much more efficient effect on crack resistance than the fine one, since the larger particle size implies a longer propagation path for cracks inside the matrix, enhancing the material deformability and, as previously mentioned, the mechanical strength.

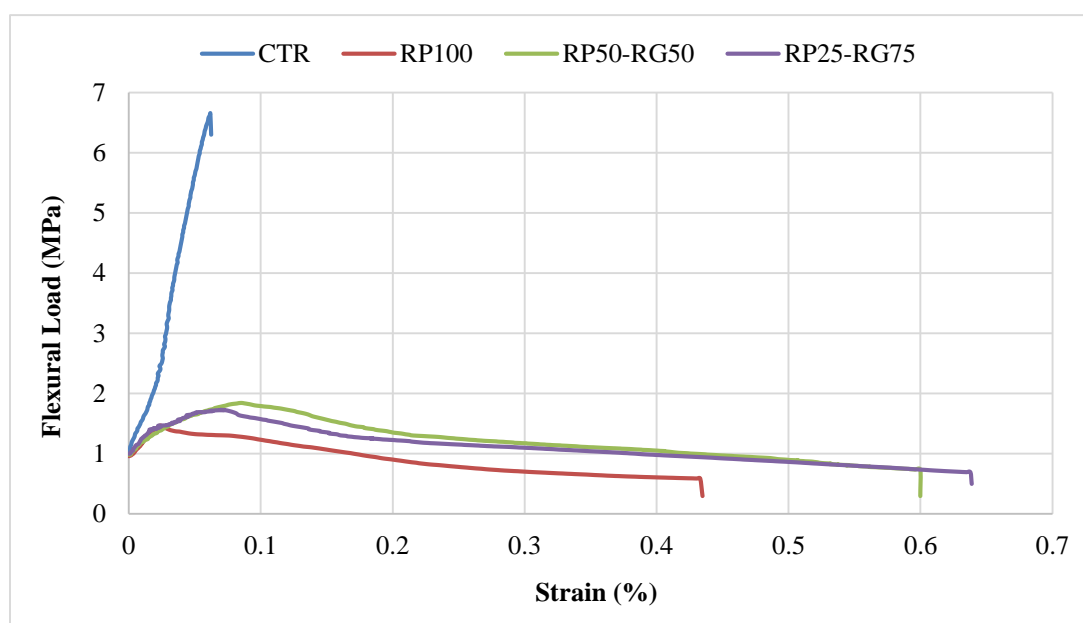


Figure 12. Load-strain diagram resulting from four-point flexural test

3.4. SIL Analysis

Figure 13 shows the *SIL* vs. *f* experimental spectra, recorded in low-middle-frequency (Figure 11a) and high-frequency (Figure 11b) bands.

Generally, for best acoustic insulation performance, a barrier material should meet specific requirements: smooth and high mass per unit area, non-porous structure, and a certain stiffness to enhance the reflection of noise wave, effectively encapsulate the incident sound, and minimize vibratory phenomena, respectively [46]. Following the characteristics listed above, it would be intuitive to deduce that the plain mortar can provide better sound-insulating behaviour than rubberized compounds. Although the modification with lightweight rubber aggregates reduces the unit weight and stiffness of the material, optimal acoustic properties are preserved. According to sound transmission theory, when the material damping is increased due to the addition of elastomeric elements, the vibro-acoustic insulation is also enhanced [47]. Besides that, additional advantages related to the versatility of lightweight cementitious materials are added: structural dead-weight reduction, thermal and fire resistance, high flexibility in fabrication and handling [48]. Globally, better attenuation performances are recorded in the high-frequency range (> 500 Hz), where the low penetrating power of the acoustic waves promotes the reflection effect of the material. Indeed, a maximum SIL-value of 21 dB was reached for the high-frequency region, while 13 dB peak-value occurred at low-middle frequency.

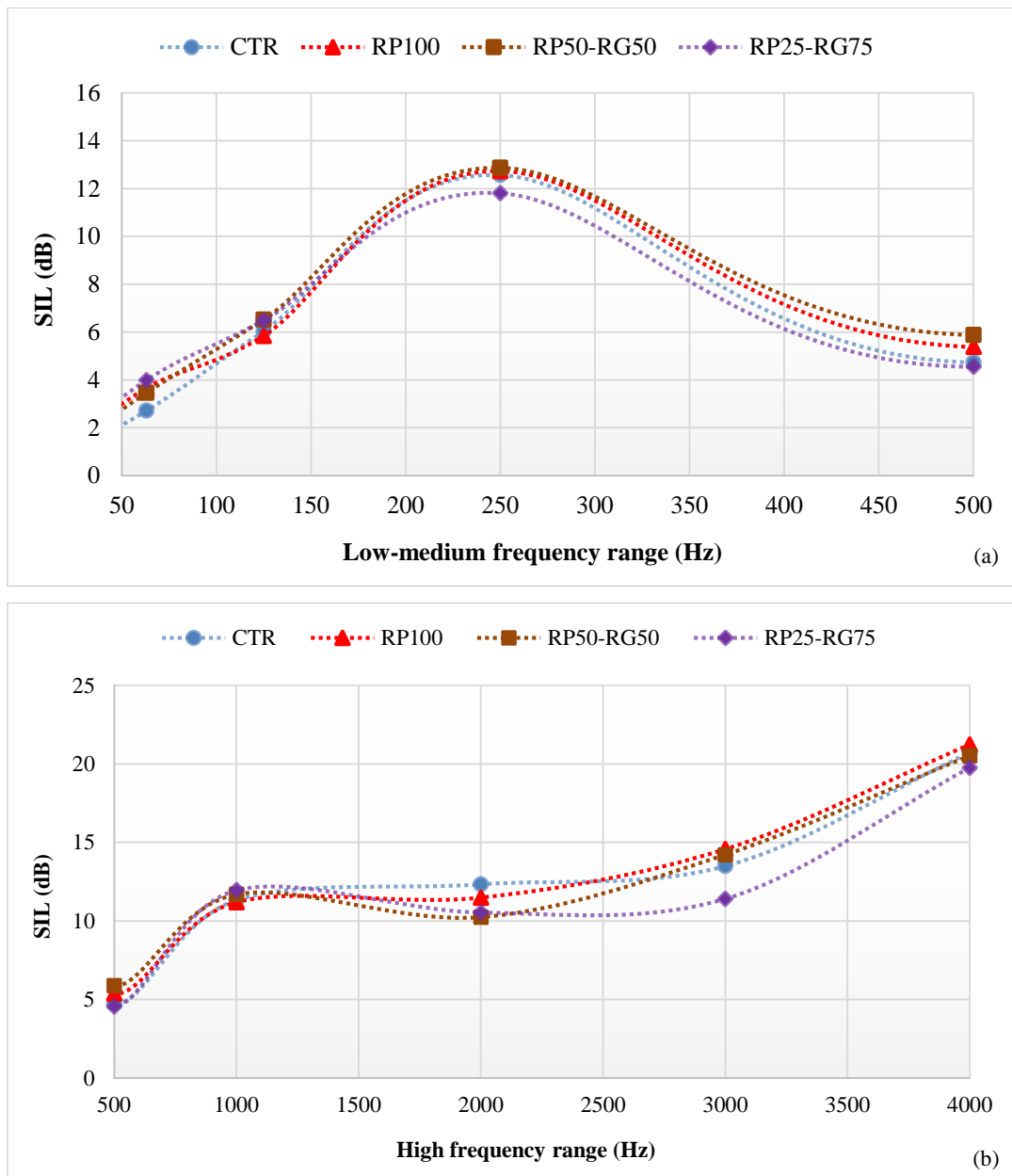


Figure 13. SIL spectrum in low-middle frequency (a) and high-frequency (b) ranges

In relation to the rubber particle size, the coarse polymer aggregates (RG), having greater inertia than fine ones, tend to dissipate higher acoustic energy rates when subjected to vibration, promoting the insulating behaviour of the material. This may explain the best acoustic performance of the RP50-RG50 in the low-middle-frequency region. However, the positive effect of RG is less in the RP25-RG75 mix, where worse acoustic properties are observed. An explanation for this evidence can be found in the porous interface between cement and RG. The increase of the percentage RG increments the presence of interfacial voids, which represent weak points for sound attenuation [49]. Above 2000 Hz, RP100 exhibits slightly superior insulation properties compared to other samples, probably due to the functional matching between microstructural homogeneity, related to RP-cement cohesion, and acoustic shielding properties.

4. Conclusions

In this research work, the microstructural, mechanical, and acoustic properties of 3D printable cement mortars modified with tire rubber aggregates deriving from ELTs were investigated. The grain size of rubber particles is a key factor in modulating the physical-mechanical behavior of the material. By considering the same sand-rubber replacement level, fine polymer fractions (RP) are preferred to obtain better adhesion with the cement matrix and greater bulk density reduction, which is related to better performance in terms of lightweight and high-frequency acoustic insulation. Conversely, coarse rubber aggregates (RG) provide a positive effect considering the lower decrease in mechanical strength, good increase in ductility, and notable sound attenuation properties at low-middle

frequency. However, their content must be correctly balanced to avoid self-defeating effects, due to the poor cohesion with the cement paste. Concerning the microstructure, an overall reduction in porosity and refinement in pore size distribution were detected in the rubberized compounds than CTR mix, implying valuable potential properties in terms of durability and thermo-acoustic performances. Regardless of the particle size, the rubber modification improves the print quality of the mixes over the plain mortar in terms of inter-layer adhesion, promoting the mechanical isotropy of the hardened material. This effect is a direct consequence of the change in rheology that rubber induces in the cementitious mixes: increasing in fresh material fluidity and appropriate conditions of surface humidity between the printed filaments. The information derived from this investigation can be potentially useful to tire recycling industry in the optimized production of rubber particles used like recycled aggregates in cementitious mixes.

Future implementations of this research will be focused on two topics:

- Improvement of rubber-cement adhesion properties to enhance the mechanical strength of the rubberized compounds. In this framework, several chemical-physical pre-treatments of rubber waste were proposed to increase the compatibilization between rubber aggregates and the cement paste [50]. It will be necessary to consider numerous aspects such as sustainability of the approach, efficiency, and compatibility with additive manufacturing technology.
- Investigate the potential technological applications of 3D printable rubber-cement mixes. The results of the experimentation conducted by the authors suggest non-structural civil and architectural applications where strength is not a priority but greater lightweight, deformability, durability and thermo-acoustic insulation properties are required. Pre-cast members including insulating bricks in masonry, noise-reducing pavements, or acoustic barriers are possible applicability ways, where the digital fabrication could bring technological benefits in terms of design freedom (production of complex functional shapes, aesthetics, and components assembly) and selective use of materials in the manufacturing.

5. Declarations

5.1. Author Contributions

Conceptualization, M.V. and M.S.; methodology, M.S.; data curation, M.V. and M.S.; writing—original draft preparation, M.S.; writing—review and editing, M.V. and M.S.; supervision, M.V. All authors have read and agreed to the published version of the manuscript.

5.2. Data Availability Statement

The data presented in this study are available in article.

5.3. Funding

This research was performed thanks to the Sapienza University direct financing for PhD student Matteo Sambucci called “Avvio alla Ricerca”. Title is: “Study and optimization of rubber-concrete additives with recycled rubber that can be used through additive manufacturing: Optimization of thermo-acoustic, rheological and mechanical properties”.

5.4. Acknowledgements

The authors express gratitude to prof. Valeria Corinaldesi and Eng. Glauco Merlonetti (Marche Polytechnic University, Italy) for their contribution to the 3D printing processes performed during the experimentation. Besides, thanks to Emaila Marmi Company (Italy) for the technical support in the cutting of the specimens for experimental characterization.

5.5. Conflicts of Interest

The authors declare no conflict of interest.

6. References

- [1] Marchment, Taylor, and Jay Sanjayan. “Mesh Reinforcing Method for 3D Concrete Printing.” *Automation in Construction* 109 (January 2020): 102992. doi:10.1016/j.autcon.2019.102992.
- [2] Yu, Shiwei, Hongjian Du, and Jay Sanjayan. “Aggregate-Bed 3D Concrete Printing with Cement Paste Binder.” *Cement and Concrete Research* 136 (October 2020): 106169. doi:10.1016/j.cemconres.2020.106169.
- [3] Ting, Guan Heng Andrew, Yi Wei Daniel Tay, Ye Qian, and Ming Jen Tan. “Utilization of Recycled Glass for 3D Concrete Printing: Rheological and Mechanical Properties.” *Journal of Material Cycles and Waste Management* 21, no. 4 (March 29, 2019): 994–1003. doi:10.1007/s10163-019-00857-x.

- [4] Valente, Marco, Abbas Sibai, and Matteo Sambucci. "Extrusion-Based Additive Manufacturing of Concrete Products: Revolutionizing and Remodeling the Construction Industry." *Journal of Composites Science* 3, no. 3 (September 4, 2019): 88. doi:10.3390/jcs3030088.
- [5] Sambucci, Matteo, Danilo Marini, Abbas Sibai, and Marco Valente. "Preliminary Mechanical Analysis of Rubber-Cement Composites Suitable for Additive Process Construction." *Journal of Composites Science* 4, no. 3 (August 18, 2020): 120. doi:10.3390/jcs4030120.
- [6] Paul, Suvash Chandra, Gideon P.A.G. van Zijl, Ming Jen Tan, and Ian Gibson. "A Review of 3D Concrete Printing Systems and Materials Properties: Current Status and Future Research Prospects." *Rapid Prototyping Journal* 24, no. 4 (May 14, 2018): 784–798. doi:10.1108/rpj-09-2016-0154.
- [7] Sambucci, Matteo, Marco Valente, Abbas Sibai, Danilo Marini, Alessia Quitadamo, and Ettore Musacchi. "Rubber-Cement Composites for Additive Manufacturing: Physical, Mechanical and Thermo-Acoustic Characterization." *Second RILEM International Conference on Concrete and Digital Fabrication (2020)*: 113–124. doi:10.1007/978-3-030-49916-7_12.
- [8] Roychand, Rajeev, Rebecca J. Gravina, Yan Zhuge, Xing Ma, Osama Youssf, and Julie E. Mills. "A Comprehensive Review on the Mechanical Properties of Waste Tire Rubber Concrete." *Construction and Building Materials* 237 (March 2020): 117651. doi:10.1016/j.conbuildmat.2019.117651.
- [9] ETRA. Available online: <https://www.etra-eu.org/> (accessed on December 2020).
- [10] Myhre, Marvin, and Duncan A. MacKillop. "Rubber Recycling." *Rubber Chemistry and Technology* 75, no. 3 (July 1, 2002): 429–474. doi:10.5254/1.3547678.
- [11] Ding, Xunhao, Tao Ma, Weiguang Zhang, and Deyu Zhang. "Experimental Study of Stable Crumb Rubber Asphalt and Asphalt Mixture." *Construction and Building Materials* 157 (December 2017): 975–981. doi:10.1016/j.conbuildmat.2017.09.164.
- [12] Siddika, Ayesha, Md. Abdullah Al Mamun, Rayed Alyousef, Y.H. Mugahed Amran, Farhad Aslani, and Hisham Alabduljabbar. "Properties and Utilizations of Waste Tire Rubber in Concrete: A Review." *Construction and Building Materials* 224 (November 2019): 711–731. doi:10.1016/j.conbuildmat.2019.07.108.
- [13] Sambucci, Matteo, Danilo Marini, and Marco Valente. "Tire Recycled Rubber for More Eco-Sustainable Advanced Cementitious Aggregate." *Recycling* 5, no. 2 (May 11, 2020): 11. doi:10.3390/recycling5020011.
- [14] Kadhim, Ali Abdulameer, and Hayder M. K. Al-Mutairee. "An Experimental Study on Behavior of Sustainable Rubberized Concrete Mixes." *Civil Engineering Journal* 6, no. 7 (July 1, 2020): 1273–1285. doi:10.28991/cej-2020-03091547.
- [15] Sambucci, M, and M Valente. "Thermal Insulation Performance Optimization of Hollow Bricks Made up of 3D Printable Rubber-Cement Mortars: Material Properties and FEM-Based Modelling." *IOP Conference Series: Materials Science and Engineering* 1044, no. 1 (January 1, 2021): 012001. doi:10.1088/1757-899x/1044/1/012001.
- [16] Valente, Marco, Matteo Sambucci, Abbas Sibai, and Ettore Musacchi. "Multi-Physics Analysis for Rubber-Cement Applications in Building and Architectural Fields: A Preliminary Analysis." *Sustainability* 12, no. 15 (July 25, 2020): 5993. doi:10.3390/su12155993.
- [17] DIN 66165-2: Particle size analysis—Sieving analysis—Part 2: procedure. DIN German Institute for Standardization: Berlin, GE (2016).
- [18] Haach, Vladimir G., Graça Vasconcelos, and Paulo B. Lourenço. "Influence of Aggregates Grading and Water/cement Ratio in Workability and Hardened Properties of Mortars." *Construction and Building Materials* 25, no. 6 (June 2011): 2980–2987. doi:10.1016/j.conbuildmat.2010.11.011.
- [19] BS 1881-114: Method for Determination of Density of Hardened Concrete. British Standard Institute: London, UK (1983).
- [20] ASTM C109/C109M-20a: Standard Test Method for Compressive Strength of Hydraulic Cement Mortars (Using 2-in. or [50-mm] Cube Specimens). ASTM International: West Conshohocken, PA, USA (2020).
- [21] ASTM C348-20: Standard Test Method for Flexural Strength of Hydraulic-Cement Mortars. ASTM International: West Conshohocken, PA, USA (2020).
- [22] EN ISO 7235:2009: Acoustics—Measurement procedures for ducted silencers—Insertion loss, flow noise and total pressure loss. EN ISO European Committee for Standardization: Bruxelles, BE (2009).
- [23] Boudaoud, Zeineddine, and Miloud Beddar. "Effects of Recycled Tires Rubber Aggregates on the Characteristics of Cement Concrete." *Open Journal of Civil Engineering* 02, no. 04 (2012): 193–197. doi:10.4236/ojce.2012.24025.
- [24] Liu, Zhongwei, Kang Zhao, Chi Hu, and Yufei Tang. "Effect of Water-Cement Ratio on Pore Structure and Strength of Foam Concrete." *Advances in Materials Science and Engineering* 2016 (2016): 1–9. doi:10.1155/2016/9520294.

- [25] Nerella, Venkatesh Naidu, Simone Hempel, and Viktor Mechtcherine. "Effects of Layer-Interface Properties on Mechanical Performance of Concrete Elements Produced by Extrusion-Based 3D-Printing." *Construction and Building Materials* 205 (April 2019): 586–601. doi:10.1016/j.conbuildmat.2019.01.235.
- [26] Ghizdăveț, Zeno, Bianca-Maria Ștefan, Daniela Nastac, Ovidiu Vasile, and Mihai Bratu. "Sound Absorbing Materials Made by Embedding Crumb Rubber Waste in a Concrete Matrix." *Construction and Building Materials* 124 (October 2016): 755–763. doi:10.1016/j.conbuildmat.2016.07.145.
- [27] Azichem. Available online: <https://www.azichem.it/news/difetti-pi%C3%B9-frequenti-nel-calcestruzzo-posato-in-opera/229> (accessed on February 2021).
- [28] Hilal, Ameer A., Nicholas Howard Thom, and Andrew Robert Dawson. "On Void Structure and Strength of Foamed Concrete Made Without/with Additives." *Construction and Building Materials* 85 (June 2015): 157–164. doi:10.1016/j.conbuildmat.2015.03.093.
- [29] Sun, Keke, Shuping Wang, Lu Zeng, and Xiaoqin Peng. "Effect of Styrene-Butadiene Rubber Latex on the Rheological Behavior and Pore Structure of Cement Paste." *Composites Part B: Engineering* 163 (April 2019): 282–289. doi:10.1016/j.compositesb.2018.11.017.
- [30] Zeng, Xiaohui, Xuli Lan, Huasheng Zhu, Haichuan Liu, Hussaini Abdullahi Umar, Youjun Xie, Guangcheng Long, and Cong Ma. "A Review on Bubble Stability in Fresh Concrete: Mechanisms and Main Factors." *Materials* 13, no. 8 (April 12, 2020): 1820. doi:10.3390/ma13081820.
- [31] Chen, Xudong, Shengxing Wu, and Jikai Zhou. "Influence of Porosity on Compressive and Tensile Strength of Cement Mortar." *Construction and Building Materials* 40 (March 2013): 869–874. doi:10.1016/j.conbuildmat.2012.11.072.
- [32] Das, B.B., and B. Kondraivendhan. "Implication of Pore Size Distribution Parameters on Compressive Strength, Permeability and Hydraulic Diffusivity of Concrete." *Construction and Building Materials* 28, no. 1 (March 2012): 382–386. doi:10.1016/j.conbuildmat.2011.08.055.
- [33] Neithalath, Narayanan, Adam Marolf, Jason Weiss, and Jan Olek. "Modeling the Influence of Pore Structure on the Acoustic Absorption of Enhanced Porosity Concrete." *Journal of Advanced Concrete Technology* 3, no. 1 (2005): 29–40. doi:10.3151/jact.3.29.
- [34] Remesar, Jose C., Sergio Vera, and Mauricio Lopez. "Assessing and Understanding the Interaction Between Mechanical and Thermal Properties in Concrete for Developing a Structural and Insulating Material." *Construction and Building Materials* 132 (February 2017): 353–364. doi:10.1016/j.conbuildmat.2016.11.116.
- [35] Weng, Yiwei, Mingyang Li, Dong Zhang, Ming Jen Tan, and Shunzhi Qian. "Investigation of Interlayer Adhesion of 3D Printable Cementitious Material from the Aspect of Printing Process." *Cement and Concrete Research* 143 (May 2021): 106386. doi:10.1016/j.cemconres.2021.106386.
- [36] Wang, Her-Yung, Bo-Tsun Chen, and Yu-Wu Wu. "A Study of the Fresh Properties of Controlled Low-Strength Rubber Lightweight Aggregate Concrete (CLSRAC)." *Construction and Building Materials* 41 (April 2013): 526–531. doi:10.1016/j.conbuildmat.2012.11.113.
- [37] Youssf, Osama, Julie E. Mills, and Reza Hassanli. "Assessment of the Mechanical Performance of Crumb Rubber Concrete." *Construction and Building Materials* 125 (October 2016): 175–183. doi:10.1016/j.conbuildmat.2016.08.040.
- [38] Wu, Yu-Fei, Syed Minhaj Saleem Kazmi, Muhammad Junaid Munir, Yingwu Zhou, and Feng Xing. "Effect of Compression Casting Method on the Compressive Strength, Elastic Modulus and Microstructure of Rubber Concrete." *Journal of Cleaner Production* 264 (August 2020): 121746. doi:10.1016/j.jclepro.2020.121746.
- [39] Habib, Ahed, Umut Yildirim, and Ozgur Eren. "Mechanical and Dynamic Properties of High Strength Concrete with Well Graded Coarse and Fine Tire Rubber." *Construction and Building Materials* 246 (June 2020): 118502. doi:10.1016/j.conbuildmat.2020.118502.
- [40] Sanjayan, Jay G., Behzad Nematollahi, Ming Xia, and Taylor Marchment. "Effect of Surface Moisture on Inter-Layer Strength of 3D Printed Concrete." *Construction and Building Materials* 172 (May 2018): 468–475. doi:10.1016/j.conbuildmat.2018.03.232.
- [41] Ma, Guowei, Yanfeng Li, Li Wang, Junfei Zhang, and Zhijian Li. "Real-Time Quantification of Fresh and Hardened Mechanical Property for 3D Printing Material by Intellectualization with Piezoelectric Transducers." *Construction and Building Materials* 241 (April 2020): 117982. doi:10.1016/j.conbuildmat.2019.117982.
- [42] Ramdani, Samiha, Abdelhamid Guettala, ML Benmalek, and José B. Aguiar. "Physical and Mechanical Performance of Concrete Made with Waste Rubber Aggregate, Glass Powder and Silica Sand Powder." *Journal of Building Engineering* 21 (January 2019): 302–311. doi:10.1016/j.job.2018.11.003.

- [43] Atahan, Ali O., and Ayhan Öner Yücel. "Crumb Rubber in Concrete: Static and Dynamic Evaluation." *Construction and Building Materials* 36 (November 2012): 617–622. doi:10.1016/j.conbuildmat.2012.04.068.
- [44] Reda Taha, M. M., A. S. El-Dieb, M. A. Abd El-Wahab, and M. E. Abdel-Hameed. "Mechanical, Fracture, and Microstructural Investigations of Rubber Concrete." *Journal of Materials in Civil Engineering* 20, no. 10 (October 2008): 640–649. doi:10.1061/(asce)0899-1561(2008)20:10(640).
- [45] Paine, K. A., and R. K. Dhir. "Research on New Applications for Granulated Rubber in Concrete." *Proceedings of the Institution of Civil Engineers - Construction Materials* 163, no. 1 (February 2010): 7–17. doi:10.1680/coma.2010.163.1.7.
- [46] Chen, Y., and N. Jiang. "Carbonized and Activated Non-Woven as High Performance Acoustic Materials: Part II Noise Insulation." *Textile Research Journal* 79, no. 3 (February 2009): 213–218. doi:10.1177/0040517508093593.
- [47] Flores Medina, Nelson, Darío Flores-Medina, and F. Hernández-Olivares. "Influence of Fibers Partially Coated with Rubber from Tire Recycling as Aggregate on the Acoustical Properties of Rubberized Concrete." *Construction and Building Materials* 129 (December 2016): 25–36. doi:10.1016/j.conbuildmat.2016.11.007.
- [48] Lo, Tommy Y., and H. Z. Cui. "Properties of green lightweight aggregate concrete." *International Workshop on Sustainable Development and Concrete Technology* (2004): 113-118.
- [49] Zhao, J., X.-M. Wang, J.M. Chang, Y. Yao, and Q. Cui. "Sound Insulation Property of Wood–waste Tire Rubber Composite." *Composites Science and Technology* 70, no. 14 (November 2010): 2033–2038. doi:10.1016/j.compscitech.2010.03.015.
- [50] Torgal, F., Shasavandi, A., and Jalali, S. "Tyre rubber wastes-based concrete: a review". *Proceedings of 1st International Conference – Wastes: Solutions, Treatments and Opportunities*. Available online: <http://hdl.handle.net/1822/14945> (accessed on February 2021).